Slab-edge modes in two-dimensional photonic crystals

Jin-Kyu Yang,[a] Se-Heon Kim, Guk-Hyun Kim, Hong-Gyu Park, and Yong-Hee Lee
Department of Physics, Korea Advanced Institute of Science and Technology, Taejon 305-701, Korea

Sung-Bock Kim
Telecommunication Basic Research Laboratory, Electronics and Telecommunications Research Institute, Taejon 305-600, Korea

(Received 16 June 2003; accepted 26 February 2004)

We demonstrate the existence of surface waves in two-dimensional photonic crystal slab edges. In finite-sized air-terminated photonic crystal boundaries, the slab-edge mode turns into a lasing mode under pulsed optical pumping conditions. Analyses of the modal behaviors of the slab-edge modes by means of calculations based on the plane wave expansion method and the finite-difference time-domain method show that resonant frequencies and quality factors are strongly dependent on the termination parameter and the shape of the slab corner. © *2004 American Institute of Physics.* [DOI: 10.1063/1.1715145]

More than half a century has passed since Kossel first studied the surface waves that exist at the interface between a periodic dielectric layer and a homogeneous material.[1] By definition, a surface wave is a propagation mode located near the interface between two material systems. Electromagnetic surface waves exist at the boundaries of photonic crystals (PCs) and propagate along the crystal–air interface.[2,3] The propagation of surface waves along the interface between air and the periodic structure of PCs is attributed to two effects: total internal reflection and the photonic bandgap (PBG) effect.[2] In two-dimensional (2D) PCs, the surface waves propagate along the truncated surface plane of the PCs.[3] The surface mode exists even at the sharply terminated edge of the freestanding 2D PC structure. Here, we name this type of surface mode as the slab-edge mode (SLEM). In this letter, we present the results of theoretical and experimental investigations of the SLEM.

We employed the three-dimensional (3D) plane wave expansion (PWE) method to study the behavior of the SLEM.[4] In order to represent the shape of the truncated slab, we introduced the termination parameter τ, which represents the shape of the truncated slab as shown in inset of Fig. 1(a). Figure 1(a) shows the dispersion characteristics of the SLEM plotted on the projected band diagram. As shown in the schematics to the right of the graph, the magnetic fields of the SLEM with $k=0.5(2\pi/a)$ are strongly confined to near the truncated slab. The dispersion curves of the SLEMs are found inside the PBG region for a wide range of τ. As the wave vector k approaches the band edge $[k=0.5(2\pi/a)]$, the slope of the dispersion curve decreases indicating that the group velocity of the mode decreases. Therefore the SLEM near the band edge is advantageous for lasing action.[5] The resonant frequencies of the PC SLEM at the band edge are plotted as a function of τ in Fig. 1(b). As τ increases, the resonant frequency of the SLEM decreases. However, the resonant frequency jumps near $\tau=0.7$, where the confined region of the mode suddenly changes from air to the dielectric material and the effective dielectric constant is changed accordingly. When $\tau=0.2$, the SLEM is found near the center of the PBG and lasing action is expected to be favored. There is another slab edge cut along the $\Gamma-M$ direction of period $\sqrt{3}\,a$. However, the SLEM was not found in this case.

To test whether the predicted SLEMs exist in real PCs, we fabricated truncated 2D slab structures of various lengths. A typical scanning electron microscope (SEM) image of the final structure is shown in Fig. 2. For preferred coupling to the TE-like modes, seven strained-compensated InGaAsP

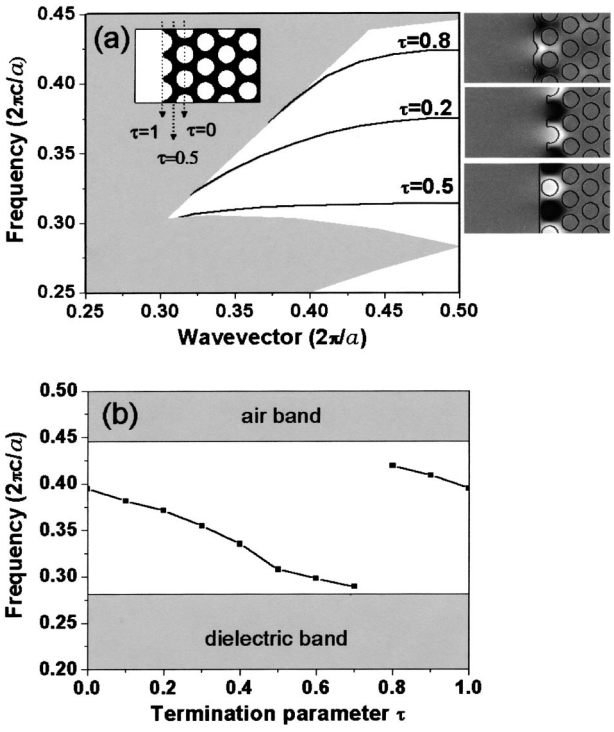

FIG. 1. SLEM predicted by 3D PWE calculations. The size of the supercell is $8\sqrt{3}\times1\times3$ with 16 plane waves per unit length. (a) Dispersion curves of various SLEMs. The inset shows the in-plane cross section of the truncated structure. The air hole radius r is $0.35\,a$ and the slab thickness d is about $0.4\,a$. The dielectric constant was set to 11.56, the value for InP materials around 1.55 μm. The images to the right of the graph show the z component of the magnetic field at the band edge $[k=0.5(2\pi/a)]$. (b) Normalized frequencies of SLEMs at the band edge.

[a]Electronic mail: jin9ya@kaist.ac.kr

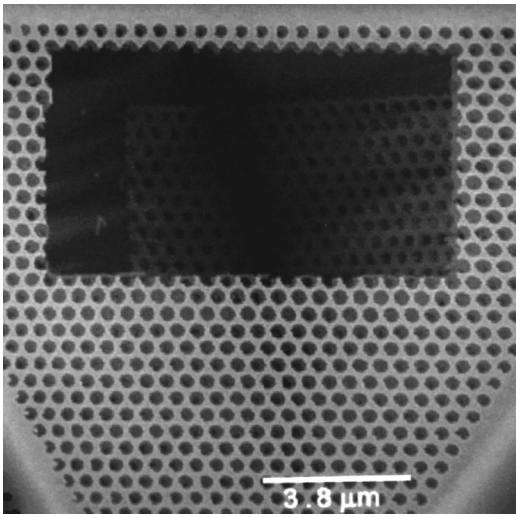

FIG. 2. SEM image of a fabricated PC slab-edge cavity sample with $a \sim 514$ nm, $r \sim 0.36\,a$, and $\tau \sim 0.27$.

quantum wells, which exhibit a photoluminescence peak near 1.55 μm, were used as the active material. The PC slab-edge structure was fabricated as follows.[6] Poly(methylmethacrylate) (PMMA) was coated on the InGaAsP/InP wafer and the PC structures were patterned using electron-beam lithography. To introduce the slab-edge structure onto the PCs, lines of closed rectangles were drawn on the PC pattern. PMMA hardened by Ar-ion bombardment was used as a mask for Ar/Cl_2 chemically assisted ion-beam etching (CAIBE). After CAIBE, the PMMA was removed by O_2 plasma and the InP membrane layer was selectively etched with a dilute $HCl:H_2O$ (4:1) solution. The resulting slab had a thickness of 200 nm, and therefore could support only fundamental slab mode.[7] In wet etching, the wafer must be turned over and carefully shaken in the dilute HCl solution. In Fig. 2, the dropped fragment is shown inside the edges, which is separated from the freestanding slab by more than the decaying length of the evanescent field. Samples with PC slab-edge lengths of $10\,a$ or $20\,a$ were fabricated.

The fabricated PC slab-edge samples were pumped by a 980 nm laser diode at room temperature. The pulse width of the pump laser was 10 ns with a 1% duty cycle because of the poor thermal conductivity of the air slab structure. A 50× microscope objective lens (numerical aperture=0.85) was used to focus the pump beam on the sample and to collect output light emitted from the PC slab edge. For polarization measurements, a polarizer was placed in front of the entrance slit of the spectrometer.

The existence of the SLEM was identified by observing the lasing action over a wide spectral range (1472–1585 nm) of the fabricated PC slab-edge structures. Typically, single fundamental mode operation was observed when the pump spot overlapped well with the length of the truncated region. However, under asymmetric pumping condition, multimode lasing was also observed sometimes. Figure 3(a) shows a typical near-field image recorded above the lasing threshold when the central region of the slab edge was optically pumped. The white dashed line represents the PC slab edge. Bright spots appear at two corners of the slab-edge structure, indicating that the guided mode is scattered to the greatest extent at corners where the SLEM encounters discontinuities. Figure 3(b) shows a typical spectrum recorded just above the lasing threshold region. The operating wavelength is 1585 nm with a threshold peak pump power of ~2 mW. As shown in Fig. 3(c), the SLEM is linearly polarized perpendicular to the line of the truncated slab, which is typical of the linear resonator.

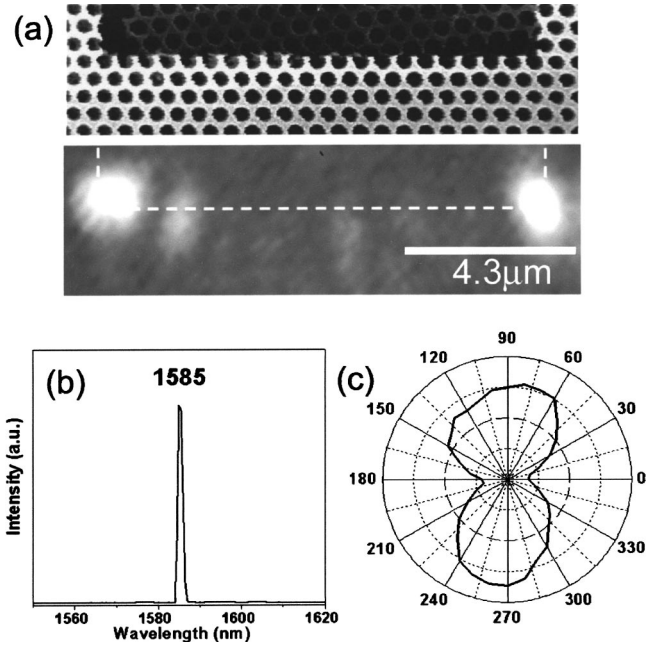

FIG. 3. Characteristics of the SLEM. (a) The upper image is a SEM image of the laser sample with $a \sim 538$ nm, $r \sim 0.35\,a$, and $\tau \sim 0.33$. The lower image is a typical near-field image above the lasing threshold captured by a CCD camera. The white dashed line shows the boundary of the slab edge. (b) A typical spectrum above the lasing threshold. (c) Polarization of the SLEM. The direction of polarization is perpendicular to the line of the truncated slab.

For finite-sized PC slab-edge structures, only those modes satisfying the resonant condition ($kL = m\pi$) can survive. As shown in the dispersion curve, the SLEM near the band edge has a smaller group velocity. Therefore, the mode nearest to the band edge is expected to have the largest effective gain. This feature is similar to the gain mechanism of the band edge laser.[5] Theoretically, the modal overlap factor of a $20\,a$-long SLEM is 9.5% similar to that of typical edge-emitting lasers. According to the 3D finite-difference time-domain (FDTD) computation,[8] the quality factor of the fundamental longitudinal SLEM (~9500) is four times larger than that of the second mode (~2100) for a $20\,a$-long slab-edge structure with $\tau = 0.2$. In other words, the fundamental mode nearest to the band edge experiences smaller optical losses. This observation agrees well with the lasing spectra, as shown in Fig. 4(a). In the spectra, sharp resonant peaks indicate longitudinal modes for a slab-edge structure. The resonant peak of the fundamental longitudinal SLEM develops into a lasing mode. Figure 4(b) shows the calculated resonant frequencies of the longitudinal fundamental SLEMs as a function of τ. According to this graph, the experimental results agree well with the FDTD results over the range of $\tau = 0.2$ to $\tau = 0.4$ within errors caused by imperfections in the fabricated PC slab. The SLEMs in other τ regions are not observed because the gain region of the active medium does not overlap with the mode frequency. To understand the near-field image above the lasing threshold, we calculated Poyn-

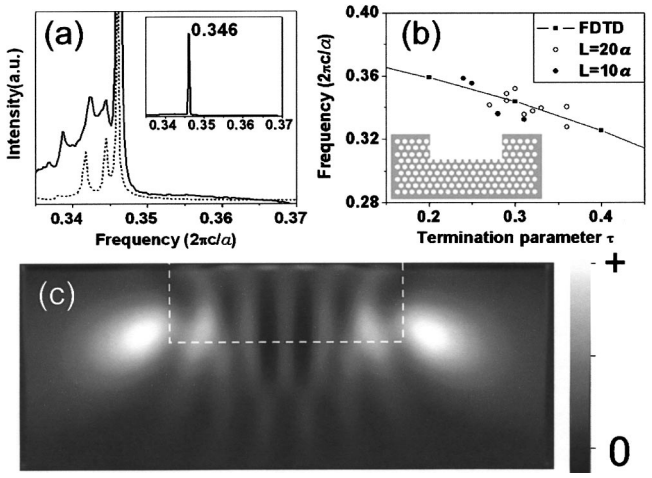

FIG. 4. (a) Theoretical (the dotted line) and experimental (the solid line) spectra for a sample in which the edge length is $20\,a$ and τ is 0.3. The inset shows the spectrum over their full intensity range. (b) Resonant frequencies of fabricated samples. The line represents the fundamental longitudinal resonant frequencies of a $10\,a$-long slab edge structure, obtained using the 3D FDTD method. The inset shows the calculated structure with $\tau=0.2$. The points mean lasing frequencies from $10\,a$-long slab edge structures (the closed circle) and $20\,a$-long slab-edge structure (the open circle). (c) The magnitude of the time-averaged Poynting vector detected in the plane with a distance of $2.5\,a$ from the surface of the slab. The white dashed line indicates the boundary of the slab edge.

ting vectors of the fundamental longitudinal SLEM. As shown in Fig. 4(c), the time-averaged Poynting vector is concentrated near the corners of the edges, which coincides with the locations at which lasing spots were observed experimentally.

To calculate the propagation loss of the SLEM and the mirror loss at the end of the finite-sized slab edge, the following equation is used:[9]

$$\frac{2\pi}{Q_{\mathrm{tot}}}\omega_n=\left(\frac{\nu_g}{c}\right)\left[a\alpha+\left(\frac{a}{L}\right)\log\left(\frac{1}{R}\right)\right]. \tag{1}$$

Here the group velocity ν_g can be obtained from the dispersion relation of the SLEM, and the mode frequency ω_n, and quality factor Q, can be obtained from the 3D FDTD calculation. The modal reflectivity depends on the corner shape of the edge. When the corner is located in the vertical line passing the center of a hole, the quality factor becomes the maximum, and the minimum when the corner is located between holes. In the case of $\tau=0.2$, the fundamental mode of $L=10\,a$ is equivalent to the second mode of $L=20\,a$ and the third mode of $L=30\,a$ with $Q_{\mathrm{tot}}\sim1200$, 2120, and 3090, respectively. From these results, the mirror reflectivity for a lattice with $a=500$ nm can be estimated to be about 87.7% and the propagation loss α to be about 12.6 dB/mm, which is more ten times smaller than the loss of the general PC waveguide mode above light line.[10] From this result, we expect the SLEM can be a candidate for a new type of the waveguide mode in PCs.

In summary, we have carried out a theoretical and experimental investigation of the 2D PC slab-edge-mode. To systematically analyze these systems, we introduced the termination parameter τ, which is defined by the shape of the truncated slab. The normalized frequency of the SLEM was found to be sensitive to the value of τ. To observe the SLEM experimentally, we fabricated the PC slab-edge structures with finite-sized edge lengths. Lasing action was observed over a wide spectral range at room temperature by optically pulsed pumping, with lasing spots appearing in the corners of the edges. Comparison of experimental data from the lasing samples with results from FDTD calculations showed that, when the normalized frequency is plotted as a function of τ, the experimental data agree well with theoretical results within errors caused by imperfections in the fabricated PC structure. The theoretical propagation loss of the SLEM is about 12.6 dB/mm at $\tau=0.2$.

This work was supported by the National Research Laboratory Project of Korea.

[1] D. Kossel, J. Opt. Soc. Am. **56**, 1464 (1969).
[2] R. D. Meade, K. D. Brommer, A. M. Rappe, and J. D. Joanopoulos, Phys. Rev. Lett. **18**, 528 (1993).
[3] F. Ramos-Mendieta and P. Halevi, Phys. Rev. B **59**, 15 112 (1999).
[4] S. G. Johnson and J. D. Joannopoulos, Opt. Express **8**, 173 (2001).
[5] J. P. Dowling, M. Scalora, M. J. Bloemer, and C. M. Bowden, J. Appl. Phys. **75**, 1896 (1994).
[6] H. Y. Ryu, S. H. Kim, S. H. Kwon, H. G. Park, and Y. H. Lee, J. Opt. Soc. Kor. **6**, 59 (2002).
[7] H. Y. Ryu, J. K. Hwang, and Y. H. Lee, J. Appl. Phys. **88**, 4941 (2000).
[8] A. Taflove, *Computational Electrodynamics: The Finite-Difference Time-Domain Method* (Artech House, Norwood, MA, 1995).
[9] S. H. Kim, H. Y. Ryu, H. G. Park, G. H. Kim, Y. S. Choi, and Y. H. Lee, Appl. Phys. Lett. **81**, 2499 (2002).
[10] M. Lončar, D. Nedeljković, T. P. Pearsall, J. Vučković, A. Scherer, S. Kuchinsky, and D. C. Allan, Appl. Phys. Lett. **80**, 1689 (2002).